J Neurophysiol 89: 2330–2333, 2003;
10.1152/jn.00764.2002.

report

Neuronal Aggregate Formation Underlies Spatiotemporal Dynamics of Nonsynaptic Seizure Initiation

Marom Bikson, John E. Fox, and John G. R. Jefferys

Department of Neurophysiology, Division of Neuroscience, University of Birmingham Medical School, Birmingham B15 2TT, United Kingdom

Submitted 14 August 2002; accepted in final form 5 December 2002

Bikson, Marom, John E. Fox, and John G. R. Jefferys. Neuronal aggregate formation underlies spatiotemporal dynamics of nonsynaptic seizure initiation. *J Neurophysiol* 89: 2330–2333, 2003; 10.1152/jn.00764.2002. High-frequency activity often precedes seizure onset. We found that electrographic seizures, induced in vitro using the low-Ca^{2+} model, start with high-frequency (>150 Hz) activity that then decreases in frequency while increasing in amplitude. Multichannel and unit recordings showed that the mechanism of this transition was the progressive formation of larger neuronal aggregates. Thus the *apparent* high-frequency activity, at seizure onset, can reflect the simultaneous recording of several slower firing aggregates. Aggregate formation rate can be accelerated by reducing osmolarity. Because synaptic transmission is blocked when extracellular Ca^{2+} is reduced, nonsynaptic mechanisms (gap junctions, field effects) must be sufficient for aggregate formation and recruitment.

INTRODUCTION

While the main phase of an epileptic attack is characterized by low-frequency (<8 Hz) rhythmic spike/sharp waves, high-frequency (40–100 Hz) activity has been observed at seizure onset, especially close to the initiation site (Allen et al. 1992; Traub et al. 2001). Several recent reports on very-high-frequency (>80 Hz) oscillations have demonstrated a critical role for nonsynaptic interactions (Draguhn et al. 1998; Towers et al. 2002; Traub et al. 2001). Under a variety of experimental conditions, nonsynaptic interactions (e.g., gap junction coupling, field effects, and ionic transients) have been shown to underlie the generation of "tonic" electrographic seizures (Demir et al. 1999; Jefferys and Haas 1982; Jensen and Yaari 1988; Konnerth et al. 1984; Patrylo et al. 1994; Pumain et al. 1985). In this report we investigated the mechanism of transition from high- to low-frequency epileptiform activity and specifically the role of nonsynaptic interactions in this transition. The results of this study suggest a novel mechanism for the generation of apparent high-frequency network activity and for the gradual transition to lower frequency epileptic discharges.

METHODS

Transverse hippocampal slices (400 μm) were prepared from male Sprague–Dawley rats (180–225 g; anesthetized with ketamine and medetomidine; killed by cervical dislocation). All efforts were made to minimize both the suffering and the number of animals tested, in accordance with UK Animal Scientific Procedures Act 1986. The slices were stored submerged in a holding chamber filled with "normal" artificial cerebrospinal fluid (ACSF) consisting of (in mM) 125 NaCl, 26 $NaHCO_3$, 3 KCl, 2 $CaCl_2$, 1.0 $MgCl_2$, 1.25 NaH_2PO_4, and 10 glucose, aerated with a 95% O_2-5% CO_2 mixture. After >60 min, slices were transferred to an interface recording chamber.

Spontaneous activity was induced by perfusion of slices with low-Ca^{2+} ACSF (35°C) consisting of (in mM) 125 NaCl, 26 $NaHCO_3$, 5 KCl, 0.2 $CaCl_2$, 1.0 $MgCl_2$, 1.25 NaH_2PO_4, and 10 glucose. Only bursts > 5 s in duration and with population spikes > 3 mV were used in this study (n = 36 slices from 23 animals). For hypoosmolar solutions, NaCl concentration was reduced to 89 mM (nominal −80 mOsm). Extracellular field potentials and units were recorded with two to four glass micropipettes (2–8 MΩ) filled with ACSF and positioned in the CA1 pyramidal cell layer. Signals were amplified and low-pass filtered (1–10 kHz) with an Axoclamp-2B or 2A (Axon Instruments, Union City, CA) and Neurolog NL-106 and NL-125 amplifiers (Digitimer, Hertfordshire, UK) and digitized using a Power 1401 and Signal software (Cambridge Electronic Design, Cambridge, UK). Analyses were performed using Spike2 (Cambridge Electronic Design) or AutoSignal (Systat Software, Richmond, CA) software. Results are reported as mean ± SD; n = number of slices.

RESULTS

Development of low-Ca^{2+} field bursts

Incubation of slices in low-Ca^{2+} ACSF (>60 min) resulted in the generation of spontaneous field bursts in the CA1 region (Jefferys and Haas 1982; Konnerth et al. 1984). Small (<400 μV) high-frequency (maximum 210 ± 82 Hz; range 85 to 370 Hz; n = 24) localized population spikes were observed at the initiation of field bursts (Fig. 1*A1*). As the burst progressed, population spike amplitude gradually increased and frequency decreased ("primary burst" minimum 28 ± 14 Hz; Fig. 1, *B* and *C*); transient increases in frequency were observed at the start of "secondary bursts." Similar results were found when frequency was quantified using autocorrelation, wavelet analysis, instantaneous frequency, or windowed average spike frequency.

Simultaneous recording from multiple sites showed that the highest peak frequencies were usually observed at sites nearest the burst initiation zone (Fig. 1*B*; 18 of 24). Population spike

Address for reprint requests: JGR Jefferys, Division of Neuroscience (Neurophysiology), University of Birmingham School of Medicine, Egbaston, Birmingham B15 2TT, UK (E-mail: J.G.R.Jefferys@bham.ac.uk).

The costs of publication of this article were defrayed in part by the payment of page charges. The article must therefore be hereby marked "*advertisement*" in accordance with 18 U.S.C. Section 1734 solely to indicate this fact.

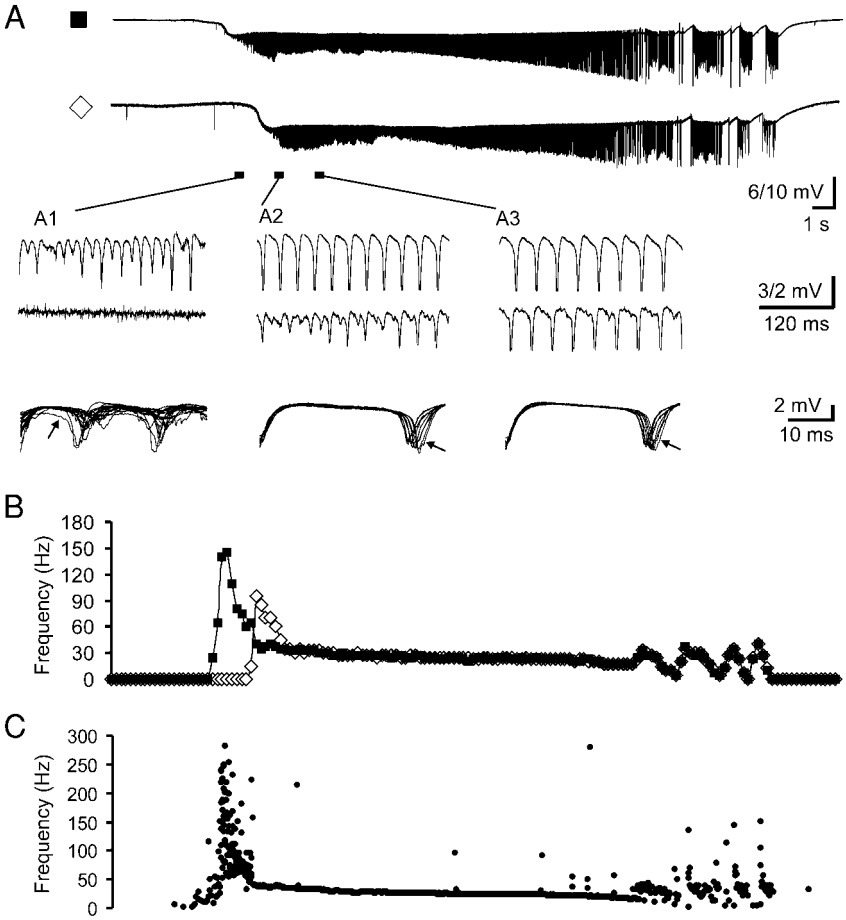

FIG. 1. Progression of population spike development during low-Ca^{2+} bursting. *A*: field burst initiated in top channel (filled square) and propagated to bottom channel (open diamond). Note that high-frequency population spikes first appeared in the top channel (*A1*). Population spike activity appeared later in the bottom channel (*A2*). As population spike amplitude increased, activity in both channels became synchronized (*A3*). *Bottom traces*: overlaid 40-ms sweeps triggered by each population spike in *A1–A3*, top channel only. Note the increased regularity in instantaneous frequency and amplitude in *A2* and *A3*; a steady decrease in frequency can still be observed. Arrows indicate the sweep triggered by the second to last population spike. *B*: plots of average population spike frequency (0.2-s window), on identical time scale to *top traces* in *A*. Leading channel (*top*), filled squares, following channel (*bottom*), open diamonds. Note the more rapid decrease in the following (open diamond) channel. *C*: plot of instantaneous frequency of population spikes > 500 μV (2–400 Hz) of the leading (*top*) channel, on identical time scale to *top traces* in *A*.

frequency in more distal areas could transiently exceed that of the initiation zone, but decreased faster and eventually "locked" into the same frequency (Fig. 1*B*). During the "locking in" period, individual population spikes in the distal channel became synchronized with those in the initiation zone (Fig. 1*A2*). The spatial extent of synchronization increased with population spike amplitude; while the initial population spike extended <0.3 mm, large (>3 mV) population spikes could propagate across the entire CA1 pyramidal cell layer (>2.5 mm).

Once synchronized (Fig. 1*A3*), population spike frequency generally continued to decrease, gradually and at a slower rate, for the duration of the field burst (Fig. 1, *A3* and *B*). In contrast, at burst onset, population spike instantaneous frequency was more variable and erratic (Fig. 1, *A1* and *C*).

Correlation of population spikes and unit activity

Previous studies, using intracellular recordings, have shown that large low-Ca^{2+} population spikes are correlated with individual pyramidal cell firing (Jefferys and Haas 1982; Taylor and Dudek 1982). In these reports, the unavoidable separation between field and intracellular recording electrodes was not critical because large population spikes are synchronized across a large area (see previous text). However, at burst initiation even a slight electrode separation could be critical because population spikes are small and highly localized.

In the present study, unit recordings from field electrodes were used to relate individual cell spiking with population spikes monitored with the same field electrode ($n = 8$; Fig. 2); thus unit and field recording are from the same neural population and there are no delays due to population spike propa-

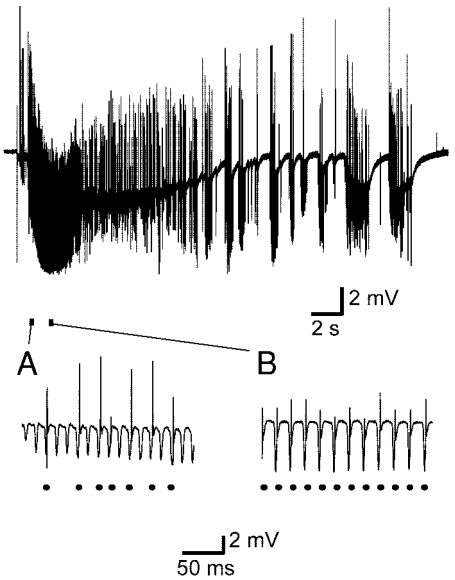

FIG. 2. Single units and population spikes recorded by a single field electrode. Population spikes appear as negative deflections. Unit spikes appear as superimposed positive deflections. *Insets*: filled circles mark unit firing times. During the early part of the field burst (*A*), the unit fired with some population spikes; as the population spike amplitude increased (*B*), the unit fired with each population spike.

gation. Early in the bursts, units fired (maximum frequency 26–92 Hz) in phase with small population spikes but not with all of them (Fig. 2*A*). As population spikes grew in amplitude, units fired with almost every population spike (Fig. 2*B*).

Modulation of burst development by osmolarity

Decreasing osmolarity (by 80 mOsm) accelerated the transition from low-amplitude, high-frequency population spikes to high-amplitude, low-frequency population spike firing (Fig. 3, *A* and *B*) and lowered the minimum discharge frequency observed during each burst ($n = 5$). In some cases, when frequencies > 40 Hz were observed >2 s after burst initiation, population spikes exhibited discrete alternating (e.g., bimodal) amplitudes (Fig. 3$A2_1$). During a burst (Fig. 3*B*, asterisk) or after osmotic challenge (compare Fig. 3, $A2_1$ and $A2_2$), a dramatic reduction in frequency (e.g., by 50%) was associated with greatly increased uniformity in population spike amplitude (see DISCUSSION). Conversely, increasing osmolarity resulted in a higher final discharge frequency (not shown, $n = 4$).

DISCUSSION

We found that high-frequency (>150 Hz) population spike activity occurred at the onset of low-Ca^{2+} bursts. These population spikes must correspond to small groups of neurons firing together in aggregates, because single-unit recordings are significantly shorter in duration and because asynchronous network activity would not be detected in a field recording. The net frequency of these initial population spikes exceeds the observed firing rate of individual units during low-Ca^{2+} bursts ($\leq$92 Hz) and therefore must represent the superimposed firing of several small neuronal aggregates (Fig. 1). The high-frequency population spikes are irregular in amplitude (Fig. 1*A1*), indicating that the number of neurons firing synchronously in each aggregate is neither uniform nor constant. Unit recordings showed that individual neurons do not necessarily fire with every small population spike (Fig. 2*A*), demonstrating variability in the composition of the aggregates contributing to successive spikes. In addition, the small population spikes are highly localized (Fig. 1), indicating that these aggregates extend over only a small region of CA1.

We propose that, as the burst develops, small individual neuronal aggregates progressively recruit one another into larger pools of neurons (Fig. 1). These larger pools generate larger population spikes (because more neurons fire synchronously) and the decrease in the number of pools firing independently results in a reduction in the *net* population spike frequency and an increase in regularity (Fig. 1, *A2* and *C*). The probability that units would fire with each population spike increases with increased population spike amplitude (Fig. 2*B*), reflecting an increase in aggregate size. This recruitment can progress until a maximum neuronal aggregate is reached. At this point, the size of the population spikes tends to plateau, because all neurons in a region have been recruited, and the correlation across the slice is high, with most of CA1 forming a single aggregate. Failure to coalesce into a single aggregate can result in a higher net frequency for the duration of the burst (Fig. 3$A2_1$).

The compound high-frequency activity, resulting from multiple aggregate firing, has a minimum interspike delay (Fig. 1*A1*) and a dominant frequency band (Fig. 3). This structure indicates that aggregate firing is not random, which may have parallels with theoretical studies on "clustering" (see Golomb and Hansel 2000). The firing frequency of individual aggregates would be a function of intrinsic membrane properties and/or the nature and strength of neuronal interactions, though not necessarily of individual aggregate size (Fig. 3$A2_1$). It is important to emphasize that the composition of individual (small) aggregates may not be fixed. The effect of osmolarity on aggregate formation could reflect an increase in neuronal excitability and/or in the strength of field effect interactions (Andrew et al. 1989; Dudek et al. 1990).

The *brief* "ripples" recorded in vitro (Draguhn et al. 1998) and in vivo near epileptic foci (Bragin et al. 2002) appear distinct from the *continuous* higher amplitude, less sharp activity reported here; however the mechanisms contributing to ripple formation are likely to promote aggregate formation. Indeed the frequency, but not amplitude or duration, of brief

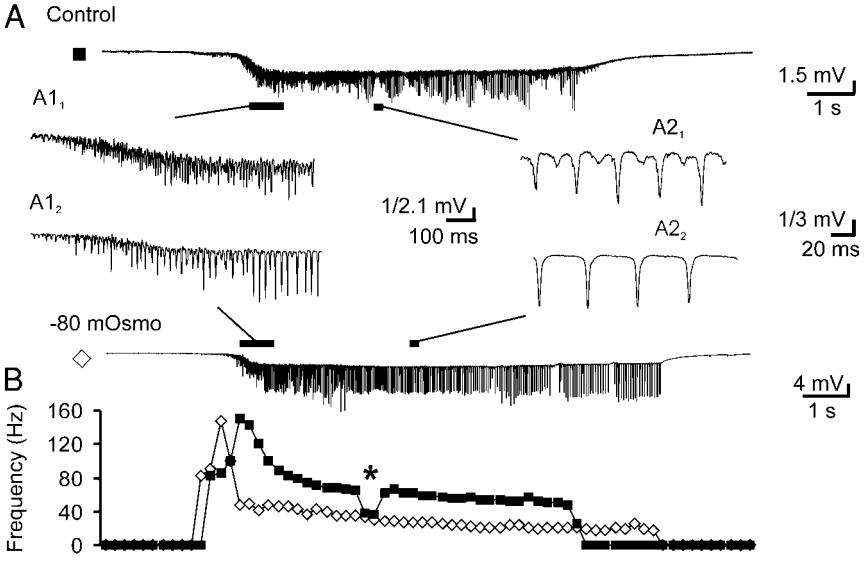

FIG. 3. Effects of reducing osmolarity on population spike dynamics. *A*: control (*top*) and hypoosmolar (*bottom*) conditions. Hypoosmolarity accelerated the growth of the population spikes and decreased their frequency (*A1*). In normal condition there appeared to be two distinct clusters of population spike size ($A2_1$). In hypoosmolar population spikes were larger and more regular in amplitude ($A2_2$). *B*: plots of population spike frequency determined by peak autocorrelation (0.2-s window) on identical time scale as full burst traces in *A*. Normal osmolar, filled squares; hypoosmolar, open diamonds.

ripples increased in the period leading up to burst initiation (not shown; $n = 3$).

We propose that the generation of high-frequency discharges results from the asynchronous firing of several neuronal aggregates, each at a lower frequency. Thus high-frequency (>40 Hz) activity recorded during clinical seizure onset could reflect the simultaneous firing of several slower oscillators. Moreover, transitions from high to low frequencies, as are observed during seizure development, could reflect the coalescence of aggregates. Consistent with this hypothesis, coherence across the hippocampal formation may increase at the start of temporal lobe seizures (Duckrow and Spencer 1992; Pacia and Ebersole 1997).

This work was supported by the Medical Research Council.

REFERENCES

Allen PJ, Fish DR, and Smith SJM. Very high-frequency rhythmic activity during SEEG suppression in frontal lobe epilepsy. *Electroencephalogr Clin Neurophysiol* 82: 155–159, 1992.

Andrew RD, Fagan M, Ballyk BA, and Rosen AS. Seizure susceptibility and the osmotic state. *Brain Res* 498: 175–180, 1989.

Bragin A, Mody I, Wilson CL, and Engel, J, Jr. Local generation of fast ripples in epileptic brain. *J Neurosci* 22: 2012–2021, 2002.

Demir R, Haberly LB, and Jackson MB. Sustained plateau activity precedes and can generate ictal-like discharges in low-Cl^- medium in slices from rat piriform cortex. *J Neurosci* 19: 10738–10746, 1999.

Draguhn A, Traub RD, Schmitz D, and Jefferys JGR. Electrical coupling underlies high-frequency oscillations in the hippocampus *in vitro*. *Nature* 394: 189–192, 1998.

Duckrow RB and Spencer SS. Regional coherence and the transfer of ictal activity during seizure onset in the medial temporal lobe. *Electroencephalogr Clin Neurophysiol* 82: 415–422, 1992.

Dudek FE, Obenaus A, and Tasker JG. Osmolality-induced changes in extracellular volume alter epileptiform bursts independent of chemical synapses in the rat: importance of non-synaptic mechanisms in hippocampal epileptogenesis. *Neurosci Lett* 120: 267–270, 1990.

Golomb D and Hansel D. The number of synaptic inputs and the synchrony of large, sparse neuronal networks. *Neural Comput* 12: 1095–1139, 2000.

Jefferys JGR and Haas HL. Synchronized bursting of CA1 pyramidal cells in the absence of synaptic transmission. *Nature* 300: 448–450, 1982.

Jensen MS and Yaari Y. The relationship between interictal and ictal paroxysms in an in vitro model of focal hippocampal epilepsy. *Ann Neurol* 24: 591–598, 1988.

Konnerth A, Heinemann U, and Yaari Y. Slow transmission of neural activity in hippocampal area CA1 in absence of active chemical synapses. *Nature* 307: 69–71, 1984.

Pacia SV and Ebersole JS. Intracranial EEG substrates of scalp ictal patterns from temporal lobe foci. *Epilepsia* 38: 642–654, 1997.

Patrylo PR, Schweitzer JS, and Dudek FE. Potassium-dependent prolonged field bursts in the dentate gyrus: effects of extracellular calcium and amino acid receptor antagonists. *Neuroscience* 61: 13–19, 1994.

Pumain R, Menini C, Heinemann U, Louvel J, and Silva-Barrat C. Chemical synaptic transmission is not necessary for epileptic seizures to persist in the baboon *Papio papio*. *Exp Neurol* 89: 250–258, 1985.

Taylor CP and Dudek FE. Synchronous neural afterdischarges in rat hippocampal slices without active chemical synapses. *Science* 218: 810–812, 1982.

Towers SK, LeBeau FE, Gloveli T, Traub RD, Whittington MA, and Buhl EH. Fast network oscillations in the rat dentate gyrus in vitro. *J Neurophysiol* 87: 1165–1168, 2002.

Traub RD, Whittington MA, Buhl EH, LeBeau FE, Bibbig A, Boyd S, Cross H, and Baldeweg T. A possible role for gap junctions in generation of very fast EEG oscillations preceding the onset of, and perhaps initiating, seizures. *Epilepsia* 42: 153–170, 2001.